

Localized polarons and doorway vibrons in finite quantum structures

H. Fehske,¹ G. Wellein,² J. Loos,³ and A. R. Bishop⁴

¹*Institut für Physik, Ernst-Moritz-Arndt-Universität Greifswald, 17487 Greifswald, Germany*

²*Regionales Rechenzentrum Erlangen, Universität Erlangen-Nürnberg, 91058 Erlangen, Germany*

³*Institute of Physics, Academy of Sciences of the Czech Republic, 16200 Prague, Czech Republic*

⁴*Theory, Simulation, and Computation Directorate, Los Alamos National Laboratory, Los Alamos, New Mexico 87545, USA*

(Received 17 October 2007; published 21 February 2008)

We consider transport through finite quantum systems such as quantum barriers, wells, dots, and junctions, coupled to local vibrational modes in the quantal regime. As a generic model, we study the Holstein-Hubbard Hamiltonian with site-dependent potentials and interactions. Depending on the barrier height to electron-phonon coupling strength ratio and the phonon frequency, we find distinctly opposed behaviors: vibration-mediated tunneling or intrinsic localization of (bi)polarons. These regimes are strongly manifested in the density correlations, mobility, and optical response calculated by exact numerical techniques.

DOI: [10.1103/PhysRevB.77.085117](https://doi.org/10.1103/PhysRevB.77.085117)

PACS number(s): 73.63.-b, 71.10.Fd, 71.38.-k, 72.10.-d

I. INTRODUCTION

Recent progress in nanotechnology has triggered a systematic study of electronic transport in microscopic systems weakly coupled to external electrodes.¹ In such devices, the active element can be a single organic molecule, but also a suspended carbon nanotube, and may be thought of as a quantum dot contacted to metallic leads that act as macroscopic charge reservoirs. In small quantum dots, energy level quantization becomes as important as electron correlations. Additionally, vibrational modes play a central role in the electron transfer through quantum dots or molecular junctions (see, e.g., the topical review of Ref. 2).

The electron-phonon (EP) interaction is found to particularly affect the dot-lead coupling. Here electronic and vibrational energies can become of the same order of magnitude, e.g., when Coulomb charging is reduced by screening due to the electrodes.³ The same circumstance holds in the polaron crossover regime, where the electrons are dressed by a phonon cloud, implying that phonon features for the current through the quantum device are of major importance.⁴ Phonon and polaron effects in nanoscale devices have been extensively discussed, e.g., for (magnetic) molecular transistors,^{3,5,6} quantum dots,⁷ tunneling diodes and Aharonov-Bohm rings,⁸ metal/organic/metal structures,⁹ and carbon nanotubes.¹⁰

In this paper, we study the electronic properties of various EP coupled quantum systems. We consider one-dimensional structures, where the “quantum device” is sandwiched between two metallic wires characterized by (tight-binding) electron hopping amplitude t , local Coulomb interaction U , and EP coupling ε_p (see Fig. 1). Such systems may be described by a generalized Holstein-Hubbard Hamiltonian. The Holstein-Hubbard model^{11–14} is not completely realistic, of course, as it only includes local electron-phonon and electron-electron interactions as well as a coupling to (dispersionless) optical phonons. However, we are interested in fundamental phenomena arising from the combination of electron-phonon interaction and “confinement” in discrete quantum structures. Besides, many aspects of finite (EP coupled) quantum systems may be understood using such simplified effective models.^{5,6,15}

II. MODEL

Allowing for site-dependent potentials and electron-phonon/electron interactions, the tight-binding Holstein-Hubbard Hamiltonian takes the form

$$H = \sum_{i,\sigma} \bar{\Delta}_i n_{i\sigma} - t \sum_{i,\sigma} (c_{i\sigma}^\dagger c_{i+1\sigma} + \text{H.c.}) + \omega_0 \sum_i b_i^\dagger b_i - \sum_{i,\sigma} \bar{g}_i \omega_0 (b_i^\dagger + b_i) n_{i\sigma} + \sum_i \bar{U}_i n_{i\uparrow} n_{i\downarrow}. \quad (1)$$

Here, $\bar{\Delta}_i = \Delta + \Delta_i$, where the potentials, Δ_i on site i , can describe a tunnel barrier, a disorder, or a voltage bias. Since we will treat left and right leads in equilibrium, we choose $\Delta = 0$ throughout the sample, neglecting a bias between the metal leads, and, in order to avoid spurious multiscattering from the boundaries in a finite system, we take periodic boundary conditions. The parameter U_i ($\bar{U}_i = U + U_i$) can be viewed as an additional Hubbard interaction or charging energy of, e.g., a quantum dot molecule. The parameter $\bar{g}_i = [(\varepsilon_p + \varepsilon_{p,i})/\omega_0]^{1/2}$ describes the local coupling of an electron on site i to an internal optical vibrational mode at the same site.¹⁶ Here, $(\varepsilon_p + \varepsilon_{p,i})$ denotes the corresponding polaron binding energy, and ω_0 is the frequency of the optical phonon.¹⁷ In this way, the model, e.g., mimics tunneling through (single or double) barriers ($\Delta_i > 0$), trapping of electrons, polarons, or bipolarons at single-impurity or double-well sites ($\Delta_i < 0$), or transport through quantum dots with soft dot-lead links.

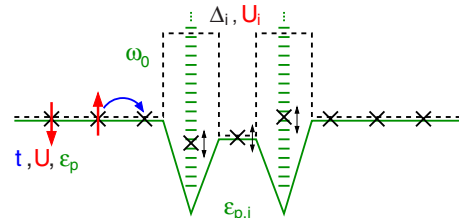


FIG. 1. (Color online) Schematic representation of model devices described by the Hamiltonian [Eq. (1)].

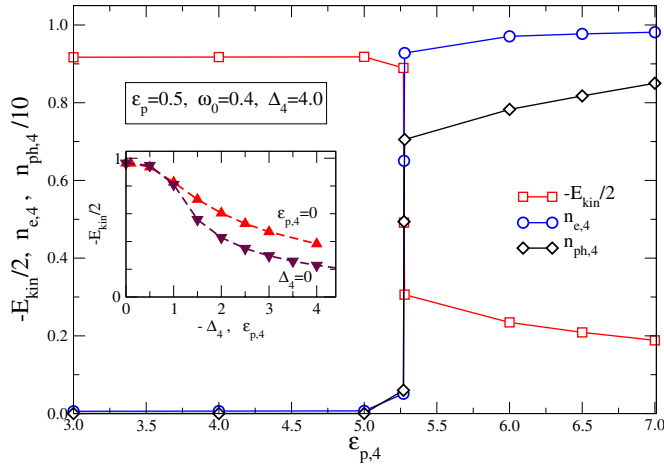


FIG. 2. (Color online) Kinetic energy of a single electron on a $N=8$ site ring with potential barrier $\Delta_4=4$ at site $i=4$. The main panel gives E_{kin} (squares), the electron density $n_{e,4}$ (circles), and the mean phonon number $n_{ph,4}$ (diamonds) at the barrier site as functions of an additional EP coupling $\varepsilon_{p,4}$. The inset shows the variation of E_{kin} if the potential Δ_4 is lowered, keeping $\varepsilon_{p,4}=0$ (triangles up) or if $\varepsilon_{p,4}$ is raised with $\Delta_4=0$ (triangles down).

On a translational invariant lattice ($\bar{\Delta}_i=\Delta$, $\bar{g}_i=g$, $\bar{U}_i=U$), the Holstein-Hubbard model can be numerically solved by variational diagonalization in the one- and two-particle sectors of interest here. This holds in the thermodynamic limit for the whole range of parameters and any dimension [for a recent review of the Holstein (bi)polaron problem, see Ref. 18]. The main result is a *continuous crossover* with increasing EP coupling strength from electronic quasiparticles weakly renormalized by phonons to (small) polarons or bipolarons.¹⁹ Depending on the value of the adiabaticity ratio $\alpha=\omega_0/t$ in one-dimensional systems, the large-to-small polaron crossover is determined by the more restrictive of the two conditions $\lambda=\varepsilon_p/2t \geq 1$ (relevant for $\alpha \ll 1$, adiabatic regime) and $g^2 \geq 1$ (for $\alpha \gg 1$, antiadiabatic regime).²⁰

Here, we address the problems of polaron/bipolaron formation and phonon-assisted transport for the more complicated *inhomogeneous* barrier structures and interactions described by the above Hamiltonian.

III. NUMERICAL RESULTS AND DISCUSSION

In our numerical work, we combine exact diagonalization (ED) and kernel polynomial methods^{21,22} to determine the ground-state and spectral properties. All energies will be measured in units of t .

A. Single-electron case

We first consider a single electron that tunnels through a *single quantum barrier*. The barrier height is assumed to considerably exceed the electron half-bandwidth. Outside the barrier, the electron is subjected to a rather moderate EP coupling, $\varepsilon_p=0.5$. The chosen phonon frequency $\omega_0=0.4$ reflects an adiabatic situation.

Figure 2 shows the behavior of the system's kinetic

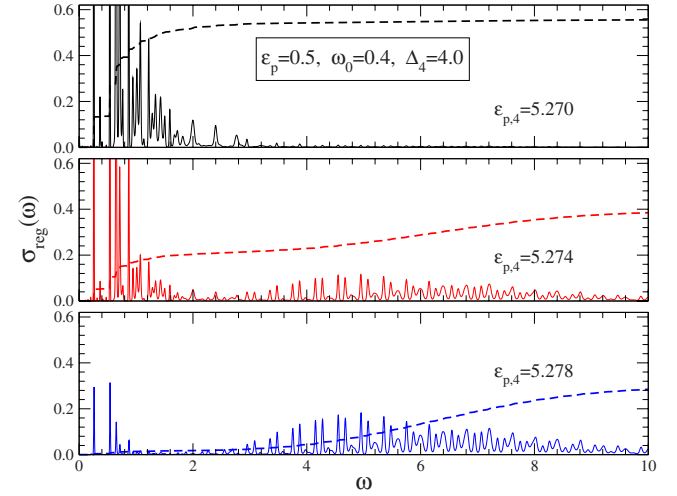


FIG. 3. (Color online) Optical response for the single-barrier system for various $\varepsilon_{p,4}$. Dashed lines give the integrated weight $S_{reg}(\omega)$.

energy

$$E_{kin} = - \sum_{i,\sigma} \langle (c_{i\sigma}^\dagger c_{i+1\sigma} + \text{H.c.}) \rangle \quad (2)$$

as the EP coupling strength is increased at the barrier site. Recall that both coherent and incoherent transport processes contribute to E_{kin} . Without loss of generality, we assume the barrier to be located at site 4. For $\varepsilon_{p,4}=0$, the barrier is almost impermeable; consequently, the local electron density $n_{e,i}=\langle n_i^\uparrow + n_i^\downarrow \rangle$ is near zero at site 4. An additional local EP interaction $\varepsilon_{p,4}$ renormalizes the on-site adiabatic potential; i.e., it leads to a local polaronic level shift that softens the barrier. Note that the kinetic energy stays almost constant until $\varepsilon_{p,4}$ exceeds a certain critical value, $\varepsilon_{p,4}^c$. At $\varepsilon_{p,4}^c$, the mobility of the electron is arrested, and the charge carrier becomes quasilocalized at the barrier site.²³ The large number of bound vibrational states ($n_{ph,4}=\langle b_4^\dagger b_4 \rangle \approx 10$) gives rise to a displaced oscillator state at site 4, i.e., a new equilibrium state of the lattice results, which lowers the energy. The *jumplike transition* is in striking contrast to what is observed if we increase only the EP coupling locally (without having a barrier) or if we form a quantum well ($\Delta_4 < 0$) without additional EP interaction (see inset of Fig. 2). In these cases we found a gradual transition from a nearly free electron to a rather immobile particle.

The extremely sharp polaron transition is accompanied by a drastic change in the optical response. The regular part of the optical conductivity is given by

$$\sigma_{reg}(\omega) = \sum_{n>0} \frac{|\langle n | \hat{j} | 0 \rangle|^2}{\omega_n} \delta(\omega - \omega_n), \quad (3)$$

where $\hat{j} = iet \sum_{i,\sigma} (c_{i\sigma}^\dagger c_{i+1\sigma} - c_{i+1\sigma}^\dagger c_{i\sigma})$ is the current operator and $|n\rangle$ represents the eigenstates of H with excitation energy $\omega_n = E_n - E_0$.

Figure 3 shows $\sigma_{reg}(\omega)$ and the integrated spectral weight

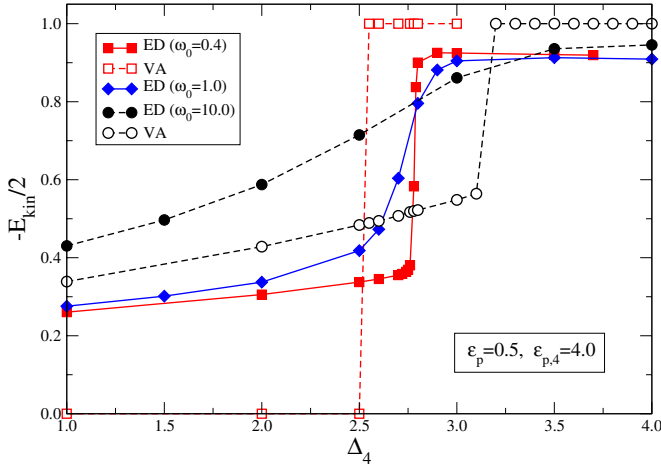


FIG. 4. (Color online) Kinetic energy upon increasing the barrier height Δ_4 at constant EP coupling. Filled (open) symbols denote ED (analytical) results for $N=8$ ($N=\infty$).

$$S_{reg}(\omega) = \int_0^\omega \sigma_{reg}(\omega') d\omega' \quad (4)$$

in the vicinity of the transition, where a tiny increase of $\varepsilon_{p,4}$ (of about 8×10^{-3} , from top to bottom) substantially changes the optical spectra. While the upper panel resembles the optical spectra of a large polaron with an absorption maximum at small frequencies and a rather asymmetric line shape, we found a bimodal signature near the transition point (middle panel) and, finally, a typical (almost symmetric) small polaron absorption just above $\varepsilon_{p,4}^c$ (lower panel). In this manner, the system acts as an optical switch.

A corresponding behavior is found if we increase the barrier (voltage bias), keeping $\varepsilon_{p,4}$ fixed (see Fig. 4). Again, the transition is “discontinuous” for small phonon frequencies, where the concept of an adiabatic energy surface holds to a good approximation. At larger phonon frequencies, nonadiabatic effects become increasingly important. Here, the EP coupling does not work against the (static) barrier directly and the transition softens as in normal polaronic systems. Furthermore, for $\omega_0 \gg 1$, the EP coupling constant \bar{g}_4 is reduced (i.e., although $\varepsilon_{p,4}$ is fixed, we leave the strong-coupling regime).

In Fig. 4, we have included the results obtained by a simple approximative analytical approach to the single-barrier problem. Assume that

$$p_j = a(R) e^{|i-j|/R}, \quad (5)$$

where $a(R) = \tanh \frac{1}{2R}$ is the probability for finding the particle at site j away from the barrier site i . Then, for the infinite system, the ground-state energy of a polaron with radius R , where $R=\infty$ corresponds to the free electron while $R=0$ describes a small polaron localized at the impurity site, is given as

$$E(R) = E_{loc}^{va} + E_{kin}^{va}, \quad (6)$$

with

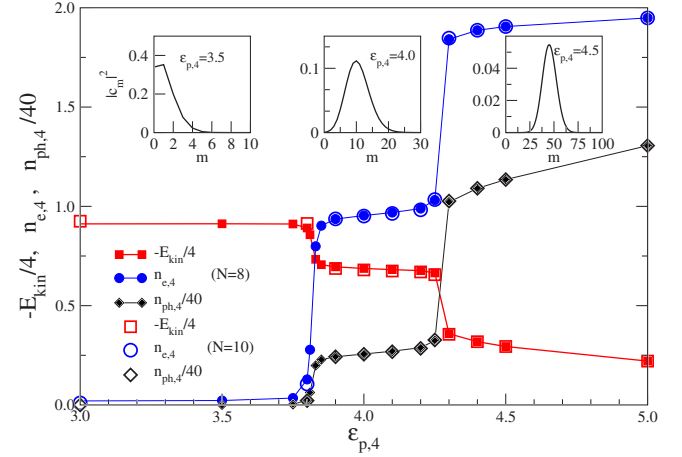


FIG. 5. (Color online) Kinetic energy (squares) and mean electron/phonon numbers (circles/diamonds) for the case of two electrons in a singlet state. We assumed a strong Hubbard interaction at the barrier ($U_4=10$, $\Delta_4=2.5$). Otherwise, $U=0$, $\varepsilon_p=0.5$, and $\omega_0=0.4$. The insets display the weight of the m -phonon state in the ground state, $|c_m|^2$, for several characteristic $\varepsilon_{p,4}$.

$$E_{loc}^{va} = \Delta_i a(R) - \omega_0 \bar{g}_i^2 a^2(R) [2 - a(R)] - 2\omega_0 g^2 a^2(R) \sum_{i \geq 1}^N e^{-2i/R} [2 - e^{-i/R} a(R)], \quad (7)$$

$$E_{kin}^{va} = -4te^{-1/2R} a(R) \left[\exp \left\{ -\frac{1}{2} a^2(R) [\bar{g}_i^2 + g^2 e^{-2/R}] \right\} + \sum_{i \geq 1}^N e^{-i/R} \exp \left\{ -\frac{1}{2} g^2 a^2(R) e^{-2i/R} [1 + e^{-2/R}] \right\} \right]. \quad (8)$$

Of course, $E(R)$ has to be minimized with respect to R . Although the kinetic energy calculated in this way neglects important contributions from multiphonon processes,²⁴ we see that E_{kin}^{va} gives a reasonable estimate for the critical value of Δ_4^c , at least in the adiabatic regime. In the antiadiabatic region, E_{kin}^{va} fails to describe the observed continuous crossover. This is a well-known shortcoming of such variational approaches, which normally yield an abrupt polaron transition in the whole frequency range.¹¹

B. Two-electron case

Next, we investigate two electrons in a single-barrier structure. Now, increasing the EP coupling on a barrier site with strong Coulomb repulsion, we found two successive transitions (see Fig. 5). In the first step, one electron becomes localized at the barrier site blocking because of the large U , the second one. Raising $\varepsilon_{p,4}$ further, both particles will be trapped, forming an on-site bipolaron. This can be seen most clearly by monitoring the density correlation

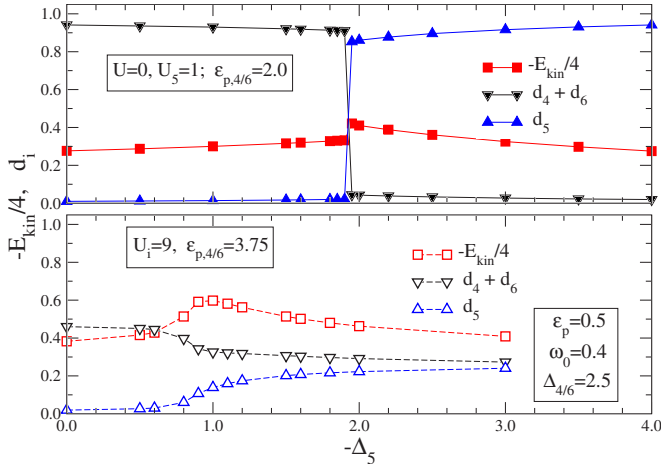


FIG. 6. (Color online) Two electrons in a quantum double-barrier system ($\Delta_{4,6}=2.5$), where the potential of the central site Δ_5 is lowered with respect to the leads (see Fig. 1). Shown are the kinetic energy (squares) and the on-site density correlations (triangles) for $\varepsilon_p=0.5$, $\omega_0=0.4$ and $U=0$, $U_5=1$ in the upper panel, while $U=9$, $U_5=0$ in the lower panel.

$$d_i = \frac{1}{4} \langle n_{e,i} + 2 \langle n_{i \uparrow} n_{i \downarrow} \rangle \rangle \quad (9)$$

as a function of the EP coupling. E_{kin} and $n_{ph,4}$ also clearly show this two-step transition, being related to significant changes of the ground-state phonon distribution,^{19,22} $|c_m|^2$ (see insets). The comparison of data for $N=8, 10$ shows that there is almost no finite-size dependence of the results.

Finally, let us consider the *double-barrier quantum dot structure* sketched in Fig. 1, with two electrons in the system. We plot in Fig. 6 the kinetic energy and the particle occupation of the barrier and embedded dot sites as functions of the depth of the quantum well ($\Delta_5 < 0$). The upper panel describes the regime of the moderate Coulomb interaction at the dot, with $U=0$ otherwise. Here, the dot is unoccupied until its potential is lowered below a critical value. Then, the particles initially located together at one of the dot-lead sites are transferred onto the dot. In this process, they change their nature from a bipolaronic quasiparticle to two electrons solely (linearly dependent) bound by the potential well (impurity). Thus, the ground state is a multiphonon (few-phonon) state for $\Delta_5 > \Delta_5^c$ ($\Delta_5 < \Delta_5^c$). If the system has a large Coulomb interaction everywhere, double occupancy is prohibited (lower panel). Then, we find initially one polaron per barrier (lead-dot) site and only one particle tunnels to the dot at Δ_5^c , thereby stripping its phonons away. Note that the mobility is enhanced in the transition region.

This effect is even more pronounced if we suppose that the EP coupling acts on the dot-lead link sites only. As can be seen from Fig. 7, there is a large jumplike increase of the particle's kinetic energy if the quantum well reaches Δ_5^c . At Δ_5^c , the bipolaron, located at one of the dot-lead link sites, dissolves and the electrons can pass over to the dot. Clearly, E_{kin} decreases if we lower the potential of the quantum dot further, but note that for $\Delta_5 < \Delta_5^c$ the kinetic energy is still *larger* than for a reference system without EP coupled dot-

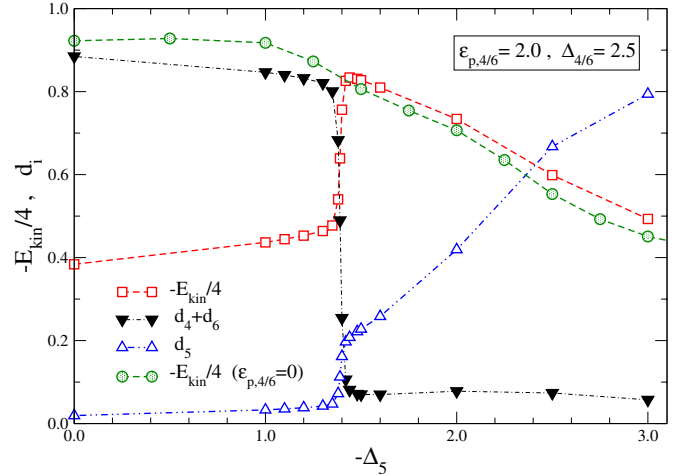


FIG. 7. (Color online) Quantum-well configuration with two electrons. The parameters are the same, as in Fig. 6 (upper panel), but now $\varepsilon_p=0$. For comparison, we show E_{kin} for a reference system without any EP coupling at the links.

lead link sites. In this way, the local coupling to vibrational degrees of freedom of the barrier opens the gate for particle transmission; i.e., vibronic excitations play the role of “doorway states.”

To corroborate the importance of these quantum lattice fluctuation effects, we determined the optical spectra below, near, and above the threshold Δ_5^c . The data presented in Fig. 8 give clear evidence for (bi)polaron hopping transport for a shallow quantum well, with dominant phonon emission and absorption processes, but resonant vibration-mediated tunneling takes place for a deeper well.

We emphasize that the increase of E_{kin} in passing below Δ_5^c is accompanied by a decrease of the total integrated weight $S_{reg}(\infty)$ of the regular (incoherent) part of $\sigma_{reg}(\omega)$ (compare dashed lines in Fig. 8 from top to bottom). Thus, exploiting the *f*-sum rule,

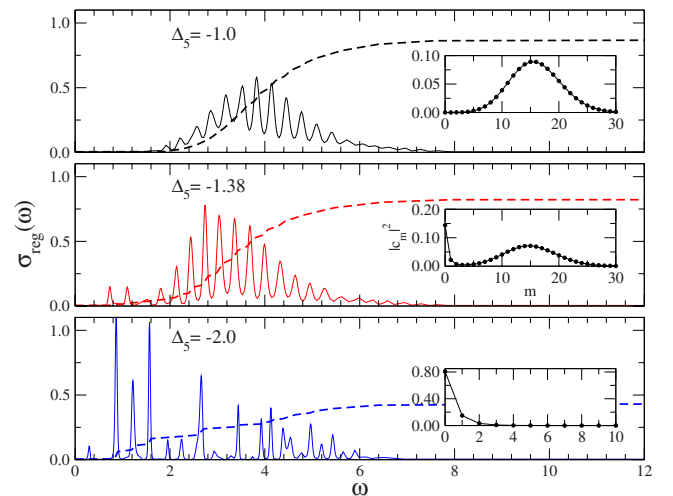


FIG. 8. (Color online) Optical conductivity for a “soft-linked” quantum dot system with two electrons (parameters as in Fig. 7). The insets give the corresponding phonon distribution functions.

$$-E_{kin}/2 = D + S_{reg}(\infty), \quad (10)$$

we can conclude that the coherent contribution (Drude part D) to E_{kin} is amplified. The insets substantiate this interpretation. Starting from a Poisson-like distribution of $|c_m|^2$, a second maximum develops at $m=0$ for $\Delta_5 \gtrsim \Delta_5^c$, and finally, for $\Delta_5 < \Delta_5^c$, the ground state contains only zero-, one-, and two-phonon states with substantial weight.

IV. SUMMARY

To conclude, investigating finite quantum structures coupled to vibronic degrees of freedom in the framework of a generalized Holstein-Hubbard Hamiltonian, we have demonstrated that interesting physics, such as intrinsic (bi)polaron localization or phonon-assisted transmission, emerges when the energy scales set by external potentials and Coulomb and electron-phonon interactions become comparable. In this regime, the interplay between the linear effects resulting from the barriers and/or cavities and the nonlinearity in-

herent in a discrete interacting electron-phonon system is of major importance. A general understanding of vibrational effects in (molecular) quantum transport, however, is still far off. Our objects in view will be to study (i) how polaronic quasiparticles time evolve when passing through phonon-coupled nanoscale structures and (ii) how finite temperature (heating) affects the balance between coherent and incoherent transport mechanisms.

ACKNOWLEDGMENTS

The authors would like to thank A. Alvermann, G. Schubert, and S. A. Trugman for useful discussions. This work was supported by DFG through SFB 512 and Grant No. 436 TSE 113/33, KONWIHR Bavaria, Academy of Sciences of the Czech Republic, and U.S. DOE. Numerical calculations were performed at LRZ Munich. H.F. and G.W. acknowledge the hospitality at the Los Alamos National Laboratory and the Institute of Physics AS CR.

-
- ¹J. Chen, M. A. Read, A. M. Rawlett, and J. M. Tour, *Science* **286**, 1550 (1990); J. Park, A. N. Pasupathy, J. L. Goldsmith, C. Chang, Y. Yaish, J. R. Petta, M. Rinkoski, J. P. Sethna, H. D. Abruña, P. L. McEuen, and D. C. Ralph, *Nature (London)* **417**, 722 (2002); J. Reichert, R. Ochs, D. Beckmann, H. B. Weber, M. Mayor, and H. v. Lohneysen, *Phys. Rev. Lett.* **88**, 176804 (2002); S. Kubatkin, A. Danilov, M. Hjort, J. Cornil, J. L. Bredas, N. Stuhr-Hansen, P. Hedegard, and T. Bjornholm, *Nature (London)* **425**, 698 (2003); H. Park, *Nat. Mater.* **6**, 330 (2007).
- ²M. Galperin, M. A. Ratner, and A. Nitzan, *J. Phys.: Condens. Matter* **19**, 103201 (2007).
- ³M. D. Nuñez Regueiro, P. S. Cornaglia, G. Usaj, and C. A. Balseiro, *Phys. Rev. B* **76**, 075425 (2007).
- ⁴A. Zazunov and T. Martin, *Phys. Rev. B* **76**, 033417 (2007).
- ⁵A. Mitra, I. Aleiner, and A. J. Millis, *Phys. Rev. B* **69**, 245302 (2004); S. Takei, Y. B. Kim, and A. Mitra, *ibid.* **72**, 075337 (2005).
- ⁶P. S. Cornaglia, D. R. Grempel, and H. Ness, *Phys. Rev. B* **71**, 075320 (2005).
- ⁷T. Inoshita and H. Sakaki, *Phys. Rev. B* **46**, 7260 (1992); S. Hameau, Y. Guldner, O. Verzellen, R. Ferreira, G. Bastard, J. Zeman, A. Lemaitre, and J. M. Gerard, *Phys. Rev. Lett.* **83**, 4152 (1999); E. A. Muljarov and R. Zimmermann, *ibid.* **93**, 237401 (2004); M. Hohenadler and H. Fehske, *J. Phys.: Condens. Matter* **19**, 255210 (2007); M. Hohenadler and P. B. Littlewood, *Phys. Rev. B* **76**, 155122 (2007).
- ⁸J. Bonča and S. A. Trugman, *Phys. Rev. Lett.* **75**, 2566 (1995); K. Haule and J. Bonča, *Phys. Rev. B* **59**, 13087 (1999).
- ⁹Z. G. Yu, D. L. Smith, A. Saxena, and A. R. Bishop, *Phys. Rev. B* **59**, 16001 (1999).
- ¹⁰B. J. LeRoy, S. G. Lemay, J. Kong, and C. Dekker, *Nature (London)* **432**, 371 (2004); X. Y. Shen, Bing Dong, X. L. Lei, and N. J. M. Horing, *Phys. Rev. B* **76**, 115308 (2007).
- ¹¹M. Deeg, H. Fehske, and H. Büttner, *Z. Phys. B: Condens. Matter* **91**, 31 (1993); U. Trapper, H. Fehske, M. Deeg, and H. Büttner, *ibid.* **93**, 465 (1993); H. Fehske, D. Ihle, J. Loos, U. Trapper, and H. Büttner, *ibid.* **94**, 91 (1994).
- ¹²J. Bonča, T. Katrašnik, and S. A. Trugman, *Phys. Rev. Lett.* **84**, 3153 (2000).
- ¹³H. Fehske, G. Wellein, G. Hager, A. Weiße, and A. R. Bishop, *Phys. Rev. B* **69**, 165115 (2004).
- ¹⁴M. Hohenadler, M. Aichhorn, and W. von der Linden, *Phys. Rev. B* **71**, 014302 (2005).
- ¹⁵L. Jacak, P. Hawrylak, and A. Wójs, *Quantum Dots* (Springer, New York, 1998).
- ¹⁶This is the basic assumption of Holstein's famous molecular crystal model [T. Holstein, *Ann. Phys. (N.Y.)* **8**, 325 (1959)]. Recall that in the case of larger molecules (e.g., quantum dots and deformable molecular transistors) the "site" index i denotes the state of the whole "entity" that couples to the vibronic mode. Importantly, although the Holstein EP interaction is local and the bare phonon frequency is dispersionless, the phonons may acquire a momentum dependence due to their coupling to the electrons.
- ¹⁷To simplify the considerations, we assume the phonon frequencies to be the same at every site, ignoring that a realistic system may be made of different materials. It is commonly accepted, however, that the polaron and bipolaron effects in quantum dots are only weakly influenced by the details by the optical phonon spectra.
- ¹⁸H. Fehske and S. A. Trugman, in *Polarons in Advanced Materials*, Springer Series in Material Sciences Vol. 103, edited by A. S. Alexandrov (Springer, New York, 2007), pp. 393–461.
- ¹⁹G. Wellein, H. Röder, and H. Fehske, *Phys. Rev. B* **53**, 9666 (1996).
- ²⁰M. Capone, W. Stephan, and M. Grilli, *Phys. Rev. B* **56**, 4484 (1997); G. Wellein and H. Fehske, *ibid.* **56**, 4513 (1997); **58**, 6208 (1998).
- ²¹B. Bäuml, G. Wellein, and H. Fehske, *Phys. Rev. B* **58**, 3663 (1998); A. Weiße, G. Wellein, A. Alvermann, and H. Fehske,

Rev. Mod. Phys. **78**, 275 (2006).

²²E. Jeckelmann and H. Fehske, Riv. Nuovo Cimento **30**, 259 (2007).

²³As a very crude estimate ($\varepsilon_p + \varepsilon_{p,4}$), has (i) to overcome the on-site potential $\Delta_4 = 4t$, and (ii) counterbalance the kinetic energy loss $2t$, i.e., taking $\varepsilon_p = 0.5t$ into account, we obtain $\varepsilon_{p,4}^c \sim 5.5t$, in

surprisingly good agreement with the exact result from Fig. 2.

²⁴The strong-coupling result for the kinetic energy of a single small polaron at the bottom of the band $E_{kin} = -(4t^2/\omega_0)\langle s^{-1} \rangle_{2g^2}$ (brackets symbolize the Poisson average with parameter $2g^2$), indicates the importance of multiphonon states.